

(–)-Tarchonanthuslactone: Design of New Analogues, Evaluation of their Antiproliferative Activity on Cancer Cell Lines, and Preliminary Mechanistic Studies

Luiz Fernando Toneto Novaes,^[a] Carolina Martins Avila,^[a] Karin Juliane Pelizzaro-Rocha,^[b] Débora Barbosa Vendramini-Costa,^[c] Marina Pereira Dias,^[b] Daniela Barreto Barbosa Trivella,^[d] João Ernesto de Carvalho,^[c] Carmen Veríssima Ferreira-Halder,^[b] and Ronaldo Aloise Pilli*^[a]

Natural products containing the α,β -unsaturated δ -lactone skeleton have been shown to possess a variety of biological activities. The natural product (–)-tarchonanthuslactone (**1**) possessing this privileged scaffold is a popular synthetic target, but its biological activity remains underexplored. Herein, the total syntheses of dihydropyran-2-ones modeled on the structure of **1** were undertaken. These compounds were obtained in overall yields of 17–21% based on the Keck asymmetric allylation reaction and were evaluated in vitro against eight different cultured human tumor cell lines. We further conducted initial investigation into the mechanism of action of selected analogues. Dihydropyran-2-one **8** [(*S,E*)-(6-oxo-3,6-dihydro-2H-pyran-2-yl)methyl 3-(3,4-dihydroxyphenyl)acrylate], a simplified

analogue of (–)-tarchonanthuslactone (**1**) bearing an additional electrophilic site and a catechol system, was the most cytotoxic and selective compound against six of the eight cancer cell lines analyzed, including the pancreatic cancer cell line. Preliminary studies on the mechanism of action of compound **8** on pancreatic cancer demonstrated that apoptotic cell death takes place mediated by an increase in the level of reactive oxygen species. It appears as though compound **8**, possessing two Michael acceptors and a catechol system, may be a promising scaffold for the selective killing of cancer cells, and thus, it deserves further investigation to determine its potential for cancer therapy.

Introduction

Natural products have been and continue to be rich sources for drug discovery with high impact especially in the development of new anticancer agents. The great structural diversity of compounds provided by nature associated with their medicinal significance has served as inspiration for the design of new lead compounds.^[1–3] In this respect, natural products displaying α,β -unsaturated δ -lactone moieties have attracted increasing interest from synthetic and medicinal chemists.^[4,5]

The α,β -unsaturated δ -lactone unit is a privileged scaffold widely distributed among natural products; it possesses a large range of biological activities, including cytotoxic activity,^[6,7] antileishmanial activity,^[8,9] anti-inflammatory activity,^[10,11]

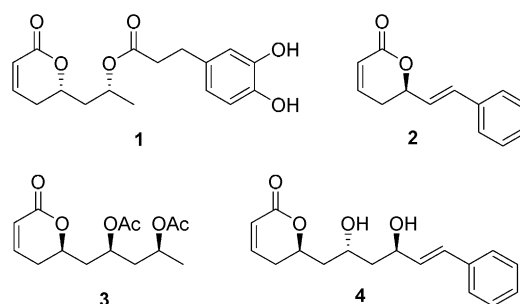


Figure 1. Chemical structures of representative natural products displaying the α,β -unsaturated δ -lactone scaffold: (–)-tarchonanthuslactone (**1**), goniothalamin (**2**), cryptocaria diacetate (**3**), and cryptomoscatone D2 (**4**).

and tubulin binding properties.^[12] The ability of the conjugated double bond to act as a Michael acceptor for biological nucleophiles features prominently in these molecules (Figure 1).^[13–15]

Tarchonanthuslactone (**1**) is a natural α,β -unsaturated δ -lactone that was first isolated by Bohlmann and Suwita in 1979 from *Tarchonanthus trilobus*.^[16] *Tarchonanthus* is a small genus occurring in the tropics and in southern Africa used in folk medicine: *T. trilobus* var. *galpinii*, also known as broad-leaved camphor bush, is used to induce vomiting and to increase libido, whereas *T. camphorata* has been used for diabetes by traditional health practitioners in Africa. Its cytotoxic and anti-inflammatory activities have also been reported.^[17]

[a] L. F. Toneto Novaes, Dr. C. Martins Avila, Prof. Dr. R. A. Pilli
Institute of Chemistry, University of Campinas (Unicamp)
C.P. 6154, 13084-971, Campinas, SP (Brazil)
E-mail: pilli@iqm.unicamp.br

[b] Dr. K. J. Pelizzaro-Rocha, M. Pereira Dias, Prof. Dr. C. V. Ferreira-Halder
Department of Biochemistry, Biology Institute
University of Campinas (Unicamp), 13083-862, Campinas, SP (Brazil)

[c] Dr. D. B. Vendramini-Costa, Prof. Dr. J. Ernesto de Carvalho
Division of Pharmacology and Toxicology—CPQBA
University of Campinas (Unicamp), 13083-970, Campinas, SP (Brazil)

[d] Dr. D. B. Barbosa Trivella
Brazilian Biosciences National Laboratory, National Center for Research in
Energy and Material, 13083-970, Campinas, SP (Brazil)

Supporting Information for this article is available on the WWW under
<http://dx.doi.org/10.1002/cmdc.201500246>.

Although tarchonanthuslactone (**1**) has become a popular synthetic target since its isolation,^[18–31] the lack of studies on its biological activity is rather surprising.^[32] Owing to our interest in investigating the cytotoxic profile of α,β -unsaturated δ -lactone inspired natural products, we devised a synthetic approach to (–)-tarchonanthuslactone (**1**) and its analogues. The synthetic strategy is based on the Keck catalytic asymmetric allylation of the aldehyde derived from (*R*)-polyhydroxybutyrate, a biorenewable starting material, followed by the construction of the dihydropyran-2-one moiety by a ring-closing metathesis reaction. A similar synthetic route was employed to access the analogues (Figure 2).

Herein, we describe the design and synthesis of analogues of (–)-tarchonanthuslactone (**1**) to evaluate key structural features related to its bioactivity regarding cancer cells. First, we investigated the effects of introducing a second electrophilic site in **1** by following an approach similar to that conducted previously with the natural product piperlongumine.^[33] A second reactive electrophilic site was introduced in (–)-tarchonanthuslactone analogue **5**, which thus generated a new α,β -unsaturated system. Further, the role of this second electrophilic site was also evaluated in compounds **6**, **8**, **10**, and **12**. Additionally, we explored the impact of the stereogenic center at C7 by using analogues **6–13**, which were also developed by targeting molecular simplification of the natural product. The R¹ and R² substituents in the aromatic ring of the simplified analogues were replaced by 3,4-dihydroxy substituents (see compounds **8** and **9**), which are present in (–)-tarchonanthuslactone (**1**) and in biologically active natural products such as caffeic acid and its derivatives,^[34,35] and by the 3,4-dimethoxy group (see compounds **10** and **11**) and the 3-methoxy-4-hydroxy group (see compounds **12** and **13**) which is present in antineoplastic agents such as combretastatin A4.^[36] Finally, we removed the α,β -unsaturated δ -lactone moiety and examined the biological profile of methyl esters **14–21** as a proof of concept of the importance of the lactone moiety (Figure 2).

Results and Discussion

Chemistry

Initially, reductive depolymerization of commercially available poly[(*R*)-3-hydroxybutyrate] (**22**) was performed upon treatment of **22** with LiAlH₄ in THF (94% yield), according to the conditions described by Seebach and Züger.^[37] Protection of the hydroxy groups of (*R*)-1,3-butanediol (**23**) with *tert*-butyldimethylsilyl (TBS) groups and selective deprotection of the primary alcohol by using HF-pyridine (HF-py) afforded mono-TBS derivative **25** in 54% overall yield. Swern oxidation of alcohol **25** furnished desired aldehyde **26** in 86% yield. Catalytic asymmetric allylation of aldehyde **26** under Keck's conditions^[38] provided homoallylic alcohol **27** in 44% yield with a diastereomeric ratio (12:1) in favor of the *syn* stereoisomer (aldehyde **26** was recovered in 28% yield). The configuration of the major isomer was established by comparison of its specific optical rotation and NMR spectroscopy data with those reported for *ent*-**26**.^[39]

The construction of α,β -unsaturated δ -lactone **30** was achieved by esterification of **27** with acryloyl chloride, followed by ring-closing metathesis by using Grubbs first-generation catalyst^[40] and deprotection of the secondary alcohol with HF-py (60% yield, three steps). With alcohol **30** in hand, (–)-tarchonanthuslactone (**1**) and corresponding analogue **5** were prepared by a sequence of esterification with the corresponding protected acids mediated by 1-ethyl-3-(3-dimethylaminopropyl)carbodiimide hydrochloride (EDC·HCl), followed by deprotection of the catechol with tetra-*n*-butylammonium fluoride (TBAF) and benzoic acid in THF (**1**, 58% yield; **5**, 50% yield) (Scheme 1). NMR spectroscopic data and the specific rotation of synthetic (–)-tarchonanthuslactone (**1**) matched those described for the natural product. The total synthesis of (–)-tarchonanthuslactone (**1**) was achieved in 10 steps in 7% overall yield.^[32]

A similar synthetic approach was employed to access simplified analogues **6–13** (Scheme 2). This time, Keck allylation of aldehyde **35** afforded homoallylic alcohol **36** in a yield higher than that observed for its superior homologue **27** (Scheme 1); whereas alcohol **27** was obtained in 44% yield accompanied

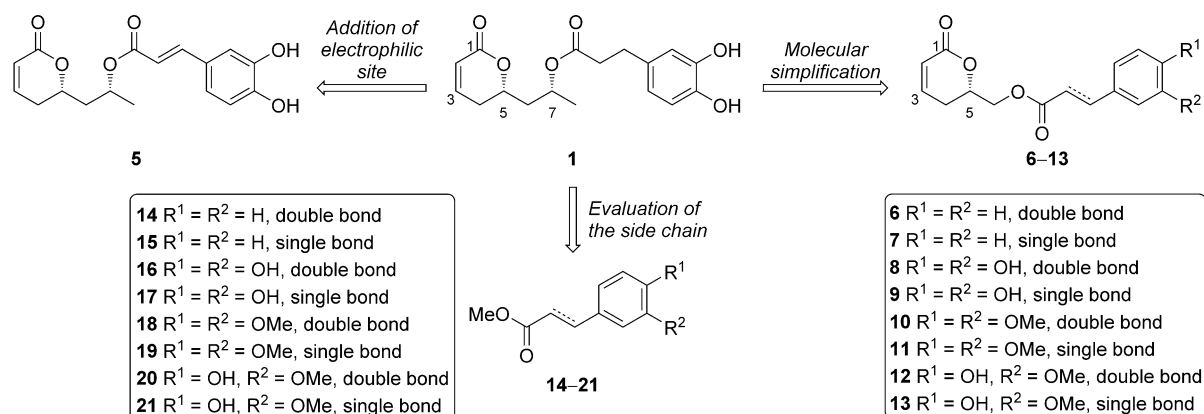
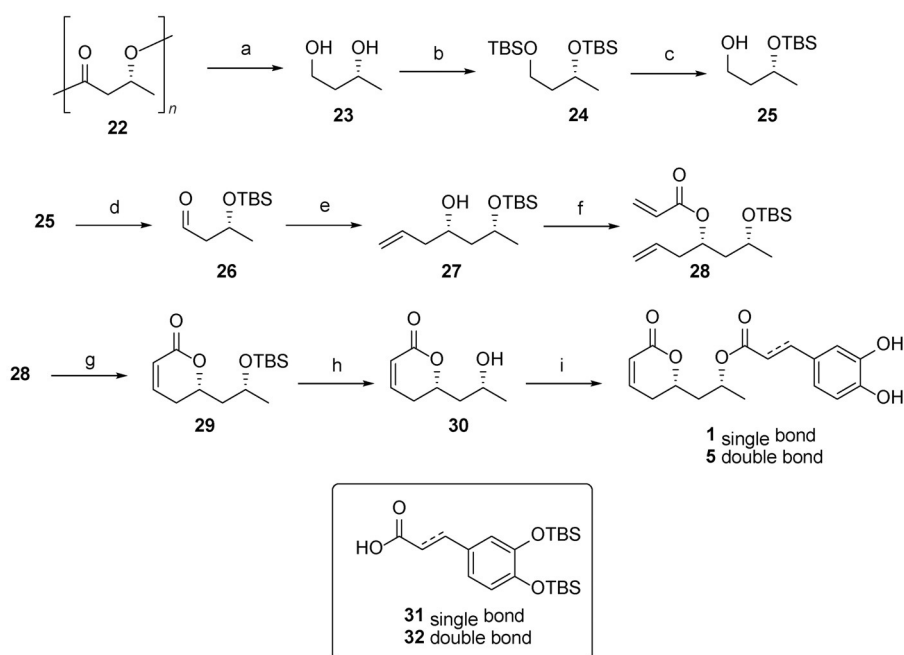
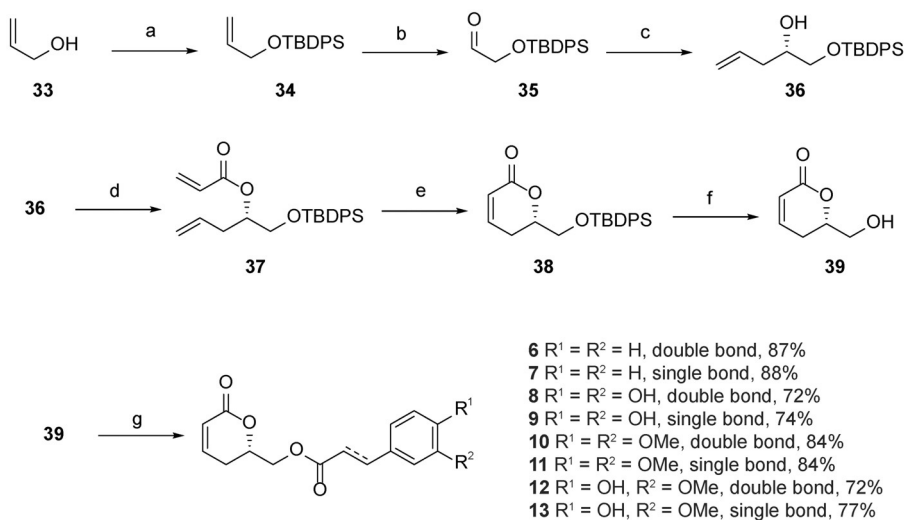


Figure 2. Design concept for analogues of (–)-tarchonanthuslactone (compounds **5–21**).



Scheme 1. Synthesis of (–)-tarchonanthuslactone (1) and analogue 5. *Reagents and conditions:* a) LiAlH_4 , THF, reflux then RT, 94%; b) TBSCl, imidazole, CH_2Cl_2 , RT, 98%; c) HF-py, pyridine, THF, RT, 55%; d) Swern oxidation, -78°C , 86%; e) 1. (S)-BINOL, $\text{Ti}(\text{O}i\text{Pr})_4$, TFA, CH_2Cl_2 , 4 Å molecular sieves, reflux; 2. $\text{Bu}_3\text{SnAllyl}$, -78 to -30°C , 44%, $dr = 12:1$; f) acryloyl chloride, Et_3N , CH_2Cl_2 , 0°C , 75%; g) Grubbs first-generation catalyst, CH_2Cl_2 , reflux, 80%; h) HF-py, pyridine, THF, RT, quant.; i) 1. **31** or **32**, EDC-HCl, DMAP, CH_2Cl_2 , RT; 2. TBAF, PhCO_2H , THF, 0°C , 58% (1) and 50% (5).



Scheme 2. Synthesis of simplified analogues of (–)-tarchonanthuslactone (1). *Reagents and conditions:* a) TBDPSCl, CH_2Cl_2 , RT, quant.; b) OsO_4 , NaIO_4 , 2,6-lutidine, H_2O , 1,4-dioxane, RT, 72%; c) 1. (S)-BINOL, $\text{Ti}(\text{O}i\text{Pr})_4$, TFA, CH_2Cl_2 , 4 Å molecular sieves, reflux; 2. $\text{Bu}_3\text{SnAllyl}$, -78 to -20°C , 87%, $er = 19:1$; d) acryloyl chloride, Et_3N , CH_2Cl_2 , 0°C , 63%; e) Grubbs first-generation catalyst, CH_2Cl_2 , reflux, 68%; f) TBAF, PhCO_2H , THF, 0°C to RT 90%; g) 1. carboxylic acid, EDC-HCl, DMAP, CH_2Cl_2 , RT; for **10–13**: 2. TBAF, PhCO_2H , THF, 0°C .

by recovery of aldehyde **26** (28%), aldehyde **35** afforded corresponding alcohol **36** in 87% yield under the same reaction conditions. The increased reactivity may be ascribed to the activated carbonyl moiety resulting from the vicinal *tert*-butyldiphenylsilyloxy (OTBDPS) group in **35**, as this activating effect is attenuated by the β -silyloxy group in **26**.

The syntheses of protected carboxylic acids **31** and **32**,^[41] derived from ferulic acid,^[41,42] and methyl esters **14–21**^[42,43] were performed by using an approach similar to that described in the literature.

Biology

Effect of (–)-tarchonanthuslactone and its analogues in cancer cell lines

To assess the differences in sensitivity displayed by each cell line to the same compound, (–)-tarchonanthuslactone (1), analogues **5–13**, and methyl esters **14–21** were evaluated in vitro against eight different cultured human tumor cell lines: glioma (U-251), breast (MCF-7), ovary expressing the multidrug resistance phenotype (NCI/ADR-RES), kidney (786-0), lung non-small cells (NCI-H460), prostate (PC-3), colon (HT-29), and pancreas (Panc-1). Additionally, the compounds were assayed in vitro against spontaneously transformed keratinocytes from histologically normal skin (HaCat cells). We further investigated the effects of the natural product and selected analogues in candidate target enzymes.

Cell growth was determined spectrophotometrically by the sulforhodamine B (SRB) assay, and the analyses were based on the U. S. National Cancer Institute (NCI) 60 tumor cell line anti-cancer drug screen (NCI60).^[44] One of the advantages of the SRB assay is the possibility to measure the cell population density at time zero (the time at which drugs are added, t_0), as this allows for the calculation of the cellular responses for total

growth inhibition (TGI). Moreover, this method displays practical advantages for large-scale screening.^[45] The TGI values were calculated from $t = t_0$, for which the amount of cells at the end of drug incubation (t), 48 h of treatment, was equal to the amount at the beginning (t_0). The compounds were assayed at concentrations between 0.16 and $250 \mu\text{g mL}^{-1}$, and

doxorubicin (DOX), employed as a positive control, at a concentration of 0.025–25 $\mu\text{g mL}^{-1}$. The results of the cancer cell line screen are summarized in Table 1.

All the compounds shown in Figure 2 were evaluated against a panel of the eight cancer cell lines listed above, but only compounds **1** and **5–13** displayed any cytotoxic effect toward U-251 (glioma), MCF-7 (breast), 786-0 (kidney), PC-3 (prostate), and Panc-1 (pancreas), and for that reason, the data for ovary cells expressing the multidrug resistance phenotype (NCI/ADR-RES), lung non-small cells (NCI-H460), and colon (HT-29) are not shown in Table 1. To start, all the dihydropyran-2-ones investigated were much less toxic to human keratinocytes (HaCat) than doxorubicin. Compound **1** exhibited antiproliferative properties against three cell lines assayed (i.e., glioma, kidney and pancreas). Selectivity of **1** to cancer cell lines was reasonable relative to transformed keratinocytes (HaCat, TGI > 100 μM).

The introduction of a second electrophilic site led to a discrete increase in the cytotoxic effect of compound **5** relative to that observed for tarchonanthuslactone (**1**), particularly for the U-251 and Panc-1 cell lines. The cytotoxic effects of compound **5** to the highly aggressive pancreas cell line Panc-1 (TGI = 23.8 μM) are more pronounced than the cytotoxic effects of compound **1** (TGI = 81.8 μM). Analogue **8** displayed a better profile for breast (MCF-7) and prostate (PC-3) relative to that shown by analogue **5**. Notably, only analogue **8** displayed any cytotoxic effect against the breast cancer cell line (MCF-7). The beneficial effect of an additional double bond with electrophilic capacity was also evident upon comparing the profiles of the pairs of compounds **6/7**, **8/9**, **10/11**, and **12/13**.

In general, simplified analogues lacking a C8–C9 olefin (i.e., compounds **7**, **9**, **11**, and **13**) were less cytotoxic in all sensitive cancer cell lines than the corresponding analogues that carry the second electrophilic site (i.e., compounds **6**, **8**, **10** and **12**).

Among the simplified analogues, compound **8** stands out as the only analogue that is effective against the breast cancer cell line (MCF-7, TGI = 27.4 μM). Furthermore, **8** retained its potency or showed enhanced potency against the other cell lines

in which the parent compounds were active. In summary, two moieties are important for the antiproliferative activity of (–)-tarchonanthuslactone derivatives: 1) the presence of the second Michael acceptor (present in compounds **5**, **6**, **8**, **10**, and **12**) and 2) the presence of the catechol system (found in compounds **8** and **9**). These two molecular features, along with structural simplification of the natural product, are combined in compound **8**, and thus, **8** is a promising scaffold for the selective killing of cancer cells.

Catechol derivatives have metal-chelating properties and can act as reducing agents.^[46,47] Additionally, catechol can undergo transformation into quinone intermediates that are able to react with cellular nucleophiles, such as the sulfhydryl groups of cysteines, to form catechol–protein conjugates.^[48] Furthermore, quinones can drive the formation of reactive oxygen species (ROS), which are capable of oxidizing several biological molecules.^[49] On the other hand, natural products with a catechol motif, for example, quercetin, possess anticancer, antioxidant, and anti-inflammatory properties.^[50]

Methyl esters **14–21** did not display significant activity (TGI > 100 μM) against the human cancer cell lines assayed. These results indicate that the α,β -unsaturated δ -lactone scaffold imparts a significant role in determining the cytotoxicity of (–)-tarchonanthuslactone analogues, as speculated previously.

Additionally, all compounds assayed have high TGI values (TGI > 100 μM) for the human keratinocytes cell line (HaCat), which reveals selectivity to cancer cells.

(–)-Tarchonanthuslactone analogues induce apoptotic cell death in pancreatic cancer cells

Recently, our research group has been interested in discovering new natural or synthetic compounds that display therapeutic potential against pancreatic cancer and in understanding their molecular mechanisms of action.^[51] Pancreatic cancer is highly aggressive and has poor prognosis. This is mainly due to the rapid development of chemoresistance to drug therapy,

Table 1. Total growth inhibition (TGI) values for (–)-tarchonanthuslactone (**1**), analogues **5–13**, and doxorubicin (DOX).^[a]

Compd	TGI [μM]						
	U-251	MCF-7	786-0	PC-3	Panc-1	HaCat	
1	58.9 ± 13.9	> 100	42.1 ± 9.2	> 100	81.8 ± 0.4	> 100	
5	20.1 ± 3.8	> 100	30.1 ± 8.7	> 100	23.8 ± 7.9	> 100	
6	19.0 ± 2.5	> 100	41.3 ± 11.8	58.1 ± 17.5	85.4 ± 0.7	> 100	
7	> 100	> 100	> 100	> 100	> 100	> 100	
8	17.6 ± 5.0	27.4 ± 12.2	31.7 ± 6.1	30.1 ± 6.1	24.6 ± 1.0	> 100	
9	28.9 ± 8.1	> 100	92.0 ± 10.8	69.4 ± 8.9	67.1 ± 5.0	> 100	
10	17.7 ± 10.6	> 100	33.1 ± 3.3	48.3 ± 9.9	25.1 ± 0.8	> 100	
11	56.6 ± 8.7	> 100	> 100	> 100	93.2 ± 22.7	> 100	
12	36.0 ± 6.0	> 100	38.9 ± 24.1	33.1 ± 16.6	23.4 ± 1.7	> 100	
13	46.7 ± 6.6	> 100	95.0 ± 4.9	> 100	95.6 ± 3.0	> 100	
DOX	0.18 ± 0.1	6.6 ± 1.2	1.9 ± 0.4	12.8 ± 1.0	28.8 ± 5.3	34.6 ± 1.4	

[a] Concentration that elicits TGI was determined from nonlinear regression analysis by using ORIGIN 8.0 (OriginLab Corporation). DOX was the positive control. Tested compounds were not effective (TGI > 100 μM) against NCI/ADR-RES, NCI-H460, and HT-29 cell lines. Test compounds were evaluated against glioma (U-251), breast (MCF-7), kidney (786-0), prostate (PC-3), and pancreas (Panc-1) cancer cell lines and transformed keratinocytes (HaCat). Results represent the average of two independent experiments performed in triplicate. Values are the mean ± SEM.

such as resistance to the chemotherapeutic agent gemcitabine, the standard drug for pancreatic cancer disease.^[52] In this context, we selected the human pancreatic carcinoma cell line (Panc-1) for additional studies among the cancer cell lines sensitized by the synthetic compounds developed herein (Table 1). The Panc-1 cell line presents higher chemoresistance to drug therapy than others pancreatic cell lines available for anticancer screening, such as BxPC-3, AsPC-1, and Mia-PaCa-2.^[53]

After the initial screening, we selected the (–)-tarchonanthuslactone analogues to evaluate their ability to induce apoptotic cell death. The experiments were performed by using double staining for annexin V and 7-aminoactinomycin D (7-AAD) and flow cytometry in Panc-1 cells. Two representative compounds were selected: simplified analogue **8**, which possesses two Michael acceptor functionalities and the catechol moiety, and corresponding analogue **9**, in which the C8=C9 double bond is removed.

Both compounds **8** and **9** were able to induce apoptotic cell death at concentrations greater than 50 μM (Figure 3a). In addition, our results clearly show that analogue **8** is more potent in inducing apoptosis than analogue **9** (100 μM , $p < 0.001$).

Currently, apoptotic cell death is the desired goal of many cancer treatments, and therefore, apoptotic inducers and regulators are considered to be of significant potential for cancer therapy.^[54] Apoptotic cell death can result from pro-apoptotic signals which are dispatched by damaged DNA or from response to oxidative stress.^[55] ROS have been considered as cytotoxic products of cellular metabolism, and the overproduction of ROS in cells may enhance cell death by apoptosis.^[56]

For this reason, we next examined whether the analogues of (–)-tarchonanthuslactone (**1**) had the ability to generate endogenous ROS in Panc-1 cells. Cells treated with analogues **8** and **9** were stained with the ROS-specific 2',7'-dichlorodihydrofluorescein diacetate (DCFH-DA) dye and were analyzed by flow cytometry. Inside the cell, nonfluorescent DCFH-DA is hydrolyzed to the polar derivative 2',7'-dichlorodihydrofluorescein (DCFH), which is oxidized in the presence of H_2O_2 to fluorescent 2',7'-dichlorofluorescein (DCF).

As observed in Figure 3b, compound **8** increased significantly the level of reactive oxygen species in Panc-1 cells, even at low concentration (25 μM). On the other hand, compound **9**, which lacks the C8–C9 olefin, was unable to elicit the same effect, as it only slightly changed the ROS levels at high concentrations (100 μM). Our results point to a positive correlation between the rate of apoptosis and the generation of ROS induced by analogue **8**.

Insight from cancer biology suggests that increasing the ROS levels may be a strategy to selectively target cancer cells.^[57–60] Previous reports have suggested that cancer cells may be particularly sensitive to ROS-modulating small molecules, especially to electrophilic small molecules.^[33,58]

ROS function as signaling molecules, and they are produced by normal cells during normal metabolic activities and are cleared by the endogenous antioxidant systems. In cancer cells, antioxidant systems are paradoxically increased, and it has been shown that these cells are strictly dependent on the antioxidant machinery.^[58,61] Cancer cells are in constant oxidative stress, which is derived from their high metabolic rate. There are at least two possible mechanisms by which small molecules can contribute to the increase in ROS levels and to the selective killing of cancer cells: 1) ROS generation by the an exogenous small molecule and 2) inhibition of the antioxidant system of the cell.^[58,59]

As mentioned above, the catechol system is known to generate radicals through its oxidation to quinones, and the latter are excellent radical stabilizers and ROS generators. Ubiquinone, in the electron-transport chain, and several natural products with antiproliferative activity (e.g., caulibugulones^[62]) are good examples of quinones that are ROS generators. ROS can oxidase several biological molecules, including DNA, proteins, and lipids, which causes cell damage and influences signaling pathways. Owing to the increased ROS levels and the extreme dependence of cancer cells to the stress machinery of ROS, the selective killing of cancer cells was observed upon perturbing the ROS balance in these cells.

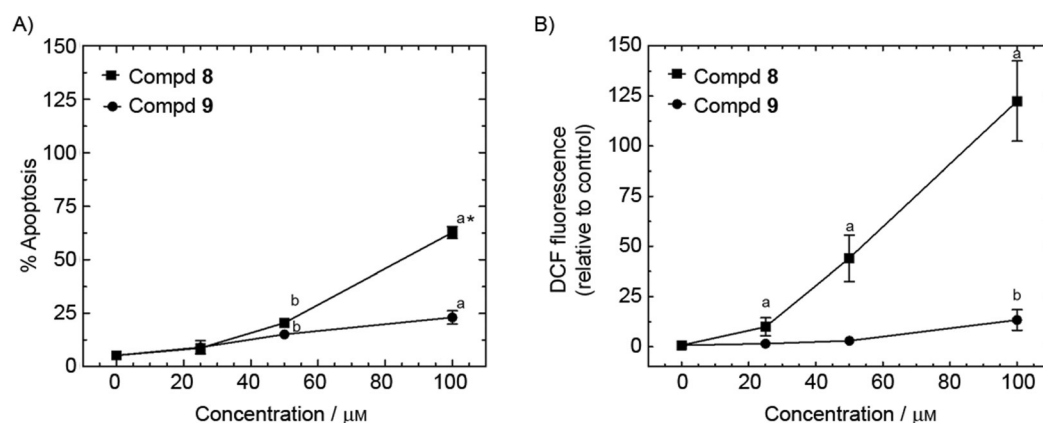


Figure 3. Measurement of apoptosis and intracellular ROS production in Panc-1 cells. Cells were treated with analogues **8** and **9** at 25, 50, and 100 μM for 24 h and then stained with a) annexin-V and 7-AAD to evaluate apoptosis and b) DCFH-DA to evaluate ROS levels. Both cells were analyzed by flow cytometry as described in the Experimental Section. Data are represented as mean \pm SEM of three independent experiments performed in duplicate. b: $p < 0.01$ versus control, a: $p < 0.001$ versus control, and *: $p < 0.001$ versus compound **9** (100 μM). Statistical analysis was assessed with ANOVA followed by Tukey test.

Our results indicate the relationship between ROS generation and Panc-1 apoptotic cell death. Therefore, we investigated possible molecular mechanisms that would lead to this phenomenon.

Protein tyrosine phosphatase inhibition and ROS generation by selected analogues of **1**

First, we investigated the inhibition of protein tyrosine phosphatase (PTPase) by selected analogues of tarchonanthuslactone (**1**). PTPases are important enzymes that play central roles in cell signaling. It has been reported that several of these enzymes are overexpressed in cancer cells.^[63] Furthermore, PTPases are known to be negatively regulated by ROS.^[64–66] In particular, some cancer cell lines overexpress the low molecular weight protein tyrosine phosphatase (LMW-PTP), and this has been correlated to the aggressiveness of these tumors.^[67] Therefore, we investigated the effects of the analogues of (–)-tarchonanthuslactone (**1**) in the activity of three representative members of PTPases, LMW-PTP, CDC-25B, and PTP-1B, all involved in cancer, and their correlation with the generation of ROS by the selected compounds (Figure 4).

We evaluated the inhibition of PTPases by selected analogues of **1** by using a standard PTPase assay. Experiments were performed with the purified enzymes and *p*-nitrophenyl phosphate as the substrate. Two pH values were selected for measuring the PTPase activity, according to their optimal pH ranges for catalytic activity. Results show that **1** and its analogues that bear the catechol system are micromolar inhibitors of CDC-25B and PTP-1B (Figure 4a).

ROS generation was measured directly from the PTPase assays. For this, we used the FOX method,^[68,69] which uses the oxidation of iron as a sensor for detecting ROS. Indeed, we observed that the compounds containing the catechol system were able to generate ROS in an alkaline medium (pH 8.2) (Figure 4b).

PTPases display an activated cysteine residue in their catalytic sites.^[70] It has been reported that oxidation of this cysteine residue can inactivate PTPases in a reversible or irreversible fashion.^[62,66] The strong correlation between the generation of ROS and the inhibition of PTPase strongly suggests that enzyme oxidation, probably induced by the generation of ROS by compounds with the catechol system, takes place. We observed in the cell assays that the presence of the catechol system in these analogues increased cell sensitivity to the compounds. Possibly, the generation of ROS by these compounds can induce enzyme oxidation in the cells, which therefore contributes to their potency.

Antioxidant machinery depletion by selected analogues of **1**

Aiming at investigating the influence of the compounds on the antioxidant machinery of cells, we also analyzed the influence of selected derivatives of **1** on the enzymatic antioxidant systems of cells. In the context of the inhibition of the antioxidant systems of cells, there are reports of small molecules interfering with the tripeptide glutathione, a known small-mole-

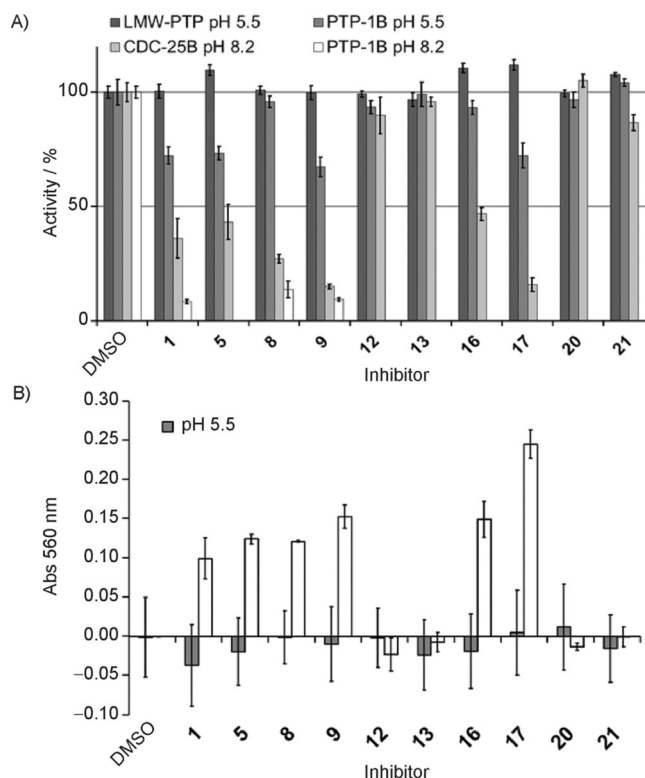


Figure 4. a) Protein tyrosine phosphatase inhibition by selected analogues of **1**; data are represented as mean \pm SD of experiments performed in triplicate. b) Generation of ROS by the compounds in the enzyme assays; data are represented as mean \pm SEM of experiments performed in duplicate. The PTPases LMW-PTP, PTP-1B, and CDC-25B were analyzed at pH 5.5 (for PTP-1B and LMW-PTP) and pH 8.2 (for CDC-25B and PTP-1B). The inhibitor concentration was 100 μ M.

cule antioxidant that plays a central role in the antioxidant system of cells. We thus measured the interaction of reduced glutathione (GSH) with analogue **8** by ¹H NMR spectroscopy (Figure 5). A solution of analogue **8** (1 mg mL⁻¹) in D₂O containing the surfactant trisaminol was treated with GSH (7 equiv) and NMR spectra were recorded every 5 min. We observed that GSH quickly performed conjugate addition to the dihydropyranone, as indicated by the complete disappearance of the signals of hydrogen atoms at C2 and C3 in the first-recorded spectrum after the addition of GSH ($t = 5$ min).

Cell-free analysis of (–)-tarchonanthuslactone analogues

Stress-related enzymes such as catalase (CAT), glutathione reductase (GR), superoxide dismutase (SOD), and glutathione-S-transferase (GST) play central roles in the antioxidant and signaling systems of cells and are considered attractive targets for cancer chemotherapy.^[58] From those, GST has been reported to act directly and indirectly in the stress response to ROS^[71,72] and, further, to be one of the enzyme targets for small molecules that selectively kill cancer cells.^[57] We, therefore, evaluated the effects of selected (–)-tarchonanthuslactone analogues in inhibiting GST in a cell-free system.

A GST inhibition assay was performed by using purified recombinant *S. japonicum* GST. First, the compounds were as-

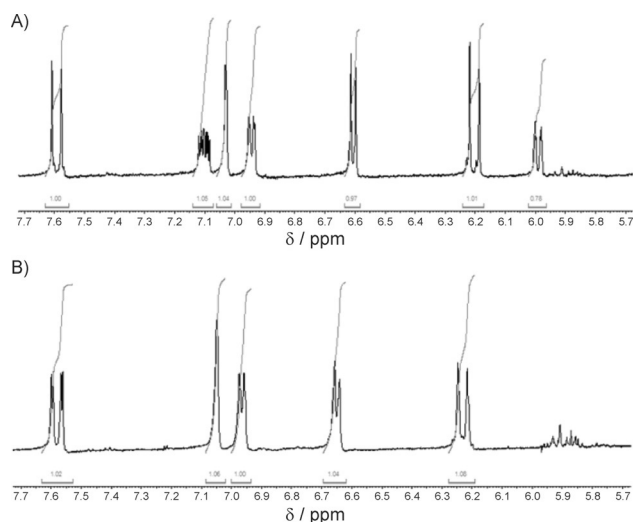


Figure 5. a) ^1H NMR spectrum (D_2O , trisaminol, 500 MHz) of analogue **8**; b) ^1H NMR spectrum (D_2O , trisaminol, 500 MHz) of analogue **8** treated with GSH after 5 min.

sayed at a single concentration (i.e., $100\ \mu\text{M}$) to select potential GST inhibitors. Subsequently, with the best inhibitors identified concentration–response curves were generated by using the concentration range of 1 to $100\ \mu\text{M}$ (Figure 6).

This assay allowed us to find GST inhibitors such as **13** with an IC_{50} value of $11\ \mu\text{M}$ and **9** with a IC_{50} of $18\ \mu\text{M}$ (Table 2). Despite the low micromolar inhibition of these analogues, there is no correlation between GST inhibition and cytotoxic activity. Therefore, we suggest that GST is not the main enzyme target of **1** and its analogues. Other studies to evaluate potential protein targets for the studied compounds are in progress.

Conclusions

The natural product (–)-tarchonanthuslactone (**1**), simplified analogues **5–13**, and methyl esters **14–21** were evaluated in vitro against eight different cultured human tumor cell lines. We also conducted an initial investigation into the mechanism of action of selected analogues. Compound **8**, which bears an additional electrophilic site relative to **1** and a catechol system, was the most cytotoxic and selective analogue of **1** evaluated. Compound **8** elicited increased sensitivity to six of the eight cancer cell lines analyzed, including pancreatic and hormone-

Table 2. IC_{50} values for in vitro GST inhibition. ^[a]	
Compd	IC_{50} [μM]
1	> 100
6	68 ± 30
7	> 100
8	≈ 100
9	18 ± 4
13	11 ± 3

[a] Data are the mean \pm SEM of at least two independent experiments performed in triplicate.

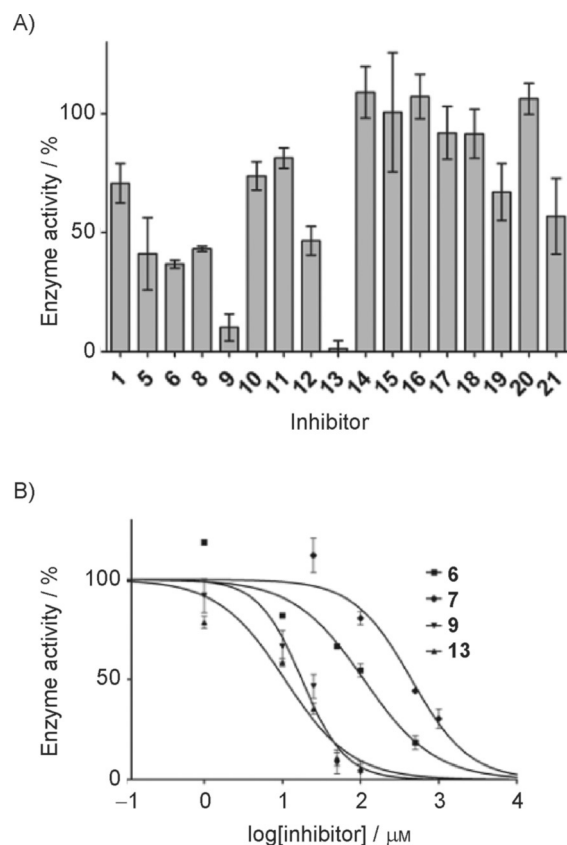


Figure 6. In vitro glutathione-S-transferase inhibition assay with selected compounds. a) GST inhibition screening with compounds at $100\ \mu\text{M}$; b) GST concentration–response curves with selected inhibitors; data are represented as mean \pm SD of experiments performed in triplicate.

induced cancer cell lines. Pancreatic cancer is one of the deadliest of the solid malignancies. Growth inhibition and induction of apoptosis constitute the major mechanisms of action of most chemotherapeutics during cancer. Unfortunately, pancreatic cancer is inherently resistant to apoptosis in all conventional cancer therapeutic agents, which poses a great challenge to clinicians for its treatment. We therefore focused on this cancer type, and a preliminary study of the mechanism of action of compound **8** in pancreatic cancer cells demonstrated that apoptotic cell death mediated by reactive oxygen species takes place.

Experimental Section

Chemistry

Starting materials and reagents were obtained from commercial sources and were used as received unless otherwise specified. Dichloromethane was treated with calcium hydride and was distilled before use. Tetrahydrofuran was treated with metallic sodium and benzophenone and was distilled before use. Anhydrous reactions were performed with continuous stirring under an atmosphere of dry nitrogen. Progress of the reactions was monitored by thin-layer chromatography (TLC) analysis (Merck, silica gel 60 F^{254} on aluminum plates). Melting points were recorded with an Electrothermal 9100 apparatus. ^1H NMR and ^{13}C NMR spectra were recorded

with Bruker 250, 400, 500, and 600 spectrometers, and the chemical shifts (δ) are reported in parts per million (ppm) relative to signals of the deuterated solvent as the internal standards (CDCl_3 $\delta_{\text{H}}=7.26$ ppm, $\delta_{\text{C}}=77.00$ ppm; $[\text{D}_6]\text{acetone}$ $\delta_{\text{H}}=2.05$ ppm, $\delta_{\text{C}}=29.92$ ppm; $[\text{D}_4]\text{methanol}$ $\delta_{\text{H}}=3.31$ ppm, $\delta_{\text{C}}=49.15$ ppm). Mass spectra were recorded with a Waters Xevo Q-ToF apparatus operating in electrospray ionization (ESI) mode. Fourier-transformed infrared (FTIR) spectra were recorded with a Thermo Scientific Nicolet i55. The specific rotations were measured at 25 °C with a PerkinElmer 341 polarimeter and a sodium lamp. The purities of the target compounds were determined by HPLC with a Waters Alliance apparatus with a C18 column (5 μm , 4.6 mm \times 150 mm), eluting with a gradient of acetonitrile and water. The preparation of tarconanthuslactone (1) and dehydro analogue 5 is described in Ref. [32].

General procedure for esterification to produce 6, 7, 10, and 11: A solution of the acid (0.63 mmol, 2 equiv) and alcohol 39 (40 mg, 0.31 mmol, 1 equiv) in anhydrous CH_2Cl_2 (2 mL) was added to a solution of EDC-HCl (119 mg, 0.63 mmol, 2 equiv) and 4-dimethylaminopyridine (DMAP; 38 mg, 0.31 mmol, 1 equiv) in anhydrous CH_2Cl_2 (9 mL) at 25 °C, and the mixture was stirred at 25 °C for 6 h. Upon completion, the mixture was diluted with EtOAc (90 mL) and extracted with an aqueous solution of 0.5 M HCl (40 mL). The organic phase was washed with an aqueous solution of saturated NaHCO_3 (30 mL), dried (MgSO_4), and concentrated. The product was purified by column chromatography (SiO_2 , hexanes/EtOAc 60:40) to afford the corresponding ester.

(S)-(6-Oxo-3,6-dihydro-2H-pyran-2-yl)methyl cinnamate (6). Yield: 70 mg (87%). White solid; $R_f=0.31$ (SiO_2 , hexanes/EtOAc 60:40); mp: 106–109 °C; $[\alpha]_{\text{D}}^{20}=-39$ ($c=1.0$ in CHCl_3); $^1\text{H NMR}$ (500 MHz, CDCl_3): $\delta=2.38\text{--}2.55$ (m, 2H), 4.41 (d, $J=4.7$ Hz, 2H), 4.58 (dq, $J=11.4$, 4.6 Hz, 1H), 6.02–6.07 (m, 1H), 6.45 (d, $J=16.0$ Hz, 1H), 6.90 (ddd, $J=9.8$, 5.9, 2.6 Hz, 1H), 7.35–7.39 (m, 3H), 7.49–7.53 (m, 2H), 7.71 ppm (d, $J=16.0$ Hz, 1H); $^{13}\text{C NMR}$ (126 MHz, CDCl_3): $\delta=25.9$, 64.7, 75.4, 117.1, 121.4, 128.2 (2C), 129.0 (2C), 130.6, 134.1, 144.6, 145.9, 163.3, 166.5 ppm; IR (KBr): $\tilde{\nu}=1168$, 1244, 1635, 1716, 2919 cm^{-1} ; HRMS: m/z : calcd for $\text{C}_{15}\text{H}_{14}\text{O}_4 + \text{H}^+$: 259.0970 $[\text{M} + \text{H}]^+$; found: 259.1020.

(S)-(6-Oxo-3,6-dihydro-2H-pyran-2-yl)methyl 3-phenylpropanoate (7). Yield: 71 mg (88%). Colorless oil; $R_f=0.31$ (SiO_2 , hexanes/EtOAc 60:40); $[\alpha]_{\text{D}}^{25}=-66$ ($c=1.0$ in CHCl_3); $^1\text{H NMR}$ (500 MHz, CDCl_3): $\delta=2.22\text{--}2.36$ (m, 2H), 2.69 (t, $J=7.6$ Hz, 2H), 2.96 (t, $J=7.6$ Hz, 2H), 4.26 (d, $J=4.6$ Hz, 2H), 4.58 (dq, $J=11.1$, 4.7 Hz, 1H), 6.00 (ddd, $J=9.8$, 2.5, 1.1 Hz, 1H), 6.85 (ddd, $J=9.8$, 5.8, 2.8 Hz, 1H), 7.17–7.22 (m, 3H), 7.26–7.30 ppm (m, 2H); $^{13}\text{C NMR}$ (126 MHz, CDCl_3): $\delta=25.5$, 30.6, 35.4, 64.4, 75.0, 120.9, 126.2, 128.2 (2C), 128.4 (2C), 140.0, 144.6, 163.1, 172.3 ppm; IR (NaCl): $\tilde{\nu}=1081$, 1104, 1161, 1246, 1389, 1454, 1497, 1604, 1732, 2951, 3028, 3062 cm^{-1} ; HRMS: m/z : calcd for $\text{C}_{15}\text{H}_{16}\text{O}_4 + \text{H}^+$: 261.1127 $[\text{M} + \text{H}]^+$; found: 261.1176.

(S,E)-(6-Oxo-3,6-dihydro-2H-pyran-2-yl)methyl 3-(3,4-dimethoxyphenyl)acrylate (10). Yield: 83 mg (84%). Colorless oil; $R_f=0.14$ (SiO_2 , hexanes/EtOAc 60:40); $[\alpha]_{\text{D}}^{25}=-26$ ($c=1.0$ in MeOH); $^1\text{H NMR}$ (500 MHz, CDCl_3): $\delta=2.37\text{--}2.53$ (m, 2H), 3.87 (s, 3H), 3.87 (s, 3H), 4.38 (d, $J=4.6$ Hz, 2H), 4.71 (dq, $J=11.4$, 4.6 Hz, 1H), 6.00–6.04 (m, 1H), 6.30 (d, $J=15.9$ Hz, 1H), 6.83 (d, $J=8.2$ Hz, 1H), 6.89 (ddd, $J=9.8$, 5.8, 2.6 Hz, 1H), 7.01 (d, $J=1.7$ Hz, 1H), 7.71 (dd, $J=8.4$, 1.8 Hz, 1H), 7.62 ppm (d, $J=15.9$ Hz, 1H); $^{13}\text{C NMR}$ (126 MHz, CDCl_3): $\delta=25.9$, 55.9, 56.0, 64.5, 75.4, 109.7, 111.1, 114.7, 121.3, 122.9, 127.1, 144.6, 145.8, 149.2, 151.4, 163.3, 166.7 ppm; IR (NaCl): $\tilde{\nu}=1140$, 1159, 1260, 1513, 1716, 2937 cm^{-1} ; HRMS: m/z : calcd for $\text{C}_{17}\text{H}_{18}\text{O}_6 + \text{H}^+$: 319.1182 $[\text{M} + \text{H}]^+$; found: 319.1221.

(S)-(6-Oxo-3,6-dihydro-2H-pyran-2-yl)methyl 3-(3,4-dimethoxyphenyl)propanoate (11). Yield: 83 mg (84%). Colorless oil; $R_f=0.11$ (SiO_2 , hexanes/EtOAc 60:40); $[\alpha]_{\text{D}}^{25}=-23$ ($c=1.0$ in MeOH); $^1\text{H NMR}$ (600 MHz, CDCl_3): $\delta=2.21\text{--}2.34$ (m, 2H), 2.64 (t, $J=7.6$ Hz, 2H), 2.87 (t, $J=7.6$ Hz, 2H), 3.81 (s, 3H), 3.83 (s, 3H), 4.24 (m, 2H), 4.57 (dq, $J=11.5$, 4.7 Hz, 1H), 5.98 (ddd, $J=9.8$, 2.5, 0.9 Hz, 1H), 6.68–6.72 (m, 2H), 6.74–6.77 (m, 1H), 6.83 ppm (ddd, $J=9.6$, 5.8, 2.6 Hz, 1H); $^{13}\text{C NMR}$ (151 MHz, CDCl_3): $\delta=25.7$, 30.4, 35.8, 55.8, 55.9, 64.5, 75.1, 111.3, 111.7, 120.2, 121.2, 132.7, 144.5, 147.5, 148.9, 163.2, 172.5 ppm; IR (NaCl): $\tilde{\nu}=1027$, 1156, 1260, 1516, 1732, 2836, 2938 cm^{-1} ; HRMS: m/z : calcd for $\text{C}_{17}\text{H}_{20}\text{O}_6 + \text{H}^+$: 321.1338 $[\text{M} + \text{H}]^+$; found: 321.1396.

General procedure for esterification and deprotection to produce 8, 9, 12, and 13: A solution of acid (0.63 mmol, 2 equiv) and alcohol 39 (40 mg, 0.31 mmol, 1 equiv) in anhydrous CH_2Cl_2 (2 mL) was added to a solution of EDC-HCl (119 mg, 0.63 mmol, 2 equiv) and DMAP (38 mg, 0.31 mmol, 1 equiv) in anhydrous CH_2Cl_2 (9 mL) at 25 °C, and the mixture was stirred at 25 °C for 6 h. Upon completion, the mixture was diluted with EtOAc (90 mL) and extracted with an aqueous solution of 0.5 M HCl (40 mL). The organic phase was washed with an aqueous saturated solution of NaHCO_3 (30 mL), dried (MgSO_4), and concentrated. The crude material was dissolved in anhydrous THF (20 mL) and benzoic acid (76 mg, 0.62 mmol, 2 equiv for 8 and 9; 38 mg, 0.31 mmol, 1 equiv for 12 and 13) and a solution of 1 M TBAF in THF (0.62 mL, 0.62 mmol, 2 equiv for 8 and 9; 0.31 mL, 0.31 mmol, 1 equiv for 12 and 13) were added at 0 °C. The mixture was stirred at this temperature for 1 h, and then an aqueous solution of 1 M HCl (30 mL) was added, and the aqueous phase was extracted with EtOAc (2 \times 60 mL). The organic phases were grouped, washed with brine (30 mL), and dried (MgSO_4). The product was purified by column chromatography (SiO_2 , hexanes/EtOAc 30:70 for 8 and 9; hexanes/EtOAc 60:40 for 12 and 13) to afford the ester.

(S,E)-(6-Oxo-3,6-dihydro-2H-pyran-2-yl)methyl 3-(3,4-dihydroxyphenyl)acrylate (8). Yield: 65 mg (72%). Brown oil; $R_f=0.44$ (SiO_2 , hexanes/EtOAc 30:70); $[\alpha]_{\text{D}}^{25}=-28$ ($c=1.0$ in MeOH); $^1\text{H NMR}$ (600 MHz, $[\text{D}_4]\text{methanol}$): $\delta=2.42\text{--}2.53$ (m, 2H), 4.37–4.40 (m, 2H), 4.77 (dq, $J=10.3$, 4.9 Hz, 1H), 4.85 (brs, 2H), 5.98–6.02 (m, 1H), 6.29 (d, $J=15.9$ Hz, 1H), 6.78 (d, $J=8.2$ Hz, 1H), 6.96 (dd, $J=8.2$, 2.1 Hz, 1H), 7.03–7.07 (m, 2H), 7.58 ppm (d, $J=15.9$ Hz, 1H); $^{13}\text{C NMR}$ (151 MHz, $[\text{D}_4]\text{methanol}$): $\delta=26.6$, 65.7, 77.3, 114.4, 115.2, 116.5, 121.2, 123.1, 127.6, 146.8, 147.6, 147.8, 149.7, 166.0, 168.6 ppm; IR (NaCl): $\tilde{\nu}=1161$, 1256, 1600, 1632, 1699, 2958, 3401 cm^{-1} (broad); HRMS: m/z : calcd for $\text{C}_{15}\text{H}_{14}\text{O}_6 + \text{H}^+$: 291.0869 $[\text{M} + \text{H}]^+$; found: 291.0971.

(S)-(6-Oxo-3,6-dihydro-2H-pyran-2-yl)methyl 3-(3,4-dihydroxyphenyl)propanoate (9). Yield: 67 mg (74%). Pale-yellow oil; $R_f=0.44$ (SiO_2 , hexanes/EtOAc 30:70); $[\alpha]_{\text{D}}^{25}=-22$ ($c=1.0$ in MeOH); $^1\text{H NMR}$ (600 MHz, $[\text{D}_4]\text{methanol}$): $\delta=2.27\text{--}2.31$ (m, 2H), 2.61 (t, $J=7.3$ Hz, 2H), 2.77 (t, $J=7.4$ Hz, 2H), 4.21 (dd, $J=12.1$, 3.6 Hz, 1H), 4.26 (dd, $J=12.2$, 5.5 Hz, 1H), 4.60 (tdd, $J=8.1$, 5.3, 3.6 Hz, 1H), 4.83 (brs, 2H), 5.95 (dt, $J=9.8$, 1.9 Hz, 1H), 6.52 (dd, $J=8.1$, 2.1 Hz, 1H), 6.64 (d, $J=2.1$ Hz, 1H), 6.66 (d, $J=7.9$ Hz, 1H), 6.96 ppm (dt, $J=9.4$, 4.3 Hz, 1H); $^{13}\text{C NMR}$ (151 MHz, $[\text{D}_4]\text{methanol}$): $\delta=26.4$, 31.3, 36.9, 65.5, 77.0, 116.4, 116.5, 120.6, 120.9, 133.3, 144.6, 146.1, 147.9, 166.0, 174.2 ppm; IR (NaCl): $\tilde{\nu}=1083$, 1114, 1260, 1446, 1520, 1604, 1716, 2958, 3315 cm^{-1} (broad); HRMS: m/z : calcd for $\text{C}_{15}\text{H}_{16}\text{O}_6 + \text{H}^+$: 293.1025 $[\text{M} + \text{H}]^+$; found: 293.1104.

(S,E)-(6-Oxo-3,6-dihydro-2H-pyran-2-yl)methyl 3-(4-hydroxy-3-methoxyphenyl)acrylate (12). Yield: 68 mg (72%). Colorless oil; $R_f=0.11$ (SiO_2 , hexanes/EtOAc 60:40); $[\alpha]_{\text{D}}^{25}=-29$ ($c=1.0$ in MeOH);

¹H NMR (500 MHz, [D₆]acetone): δ = 2.52–2.56 (m, 2H), 3.92 (s, 3H), 4.39 (d, J = 4.9 Hz, 2H), 4.74–4.81 (m, 1H), 5.97 (dt, J = 9.8, 1.8 Hz, 1H), 6.44 (d, J = 16.0 Hz, 1H), 6.88 (d, J = 8.1 Hz, 1H), 7.05 (ddd, J = 9.8, 4.4, 4.1 Hz, 1H), 7.15 (dd, J = 8.1, 1.8 Hz, 1H), 7.36 (d, J = 1.8 Hz, 1H), 7.65 ppm (d, J = 15.9 Hz, 1H); ¹³C NMR (126 MHz, [D₆]acetone): δ = 26.3, 56.3, 65.3, 76.3, 111.2, 111.3, 115.1, 116.0, 121.3, 124.2, 127.3, 146.5, 148.7, 150.1, 163.6, 167.2 ppm; IR (NaCl): $\tilde{\nu}$ = 1159, 1515, 1711, 3400 cm⁻¹ (broad); HRMS: m/z : calcd for C₁₆H₁₆O₆ + H⁺: 305.1025 [M + H]⁺; found: 305.1090.

(S)-(6-Oxo-3,6-dihydro-2H-pyran-2-yl)methyl 3-(4-hydroxy-3-methoxyphenyl)propanoate (13). Yield: 73 mg (77%). Colorless oil; R_f = 0.11 (SiO₂, hexanes/EtOAc 60:40); [α]_D²⁵ = -22 (c = 1.0 in MeOH); ¹H NMR (600 MHz, CDCl₃): δ = 2.21–2.33 (m, 2H), 2.64 (t, J = 7.6 Hz, 2H), 2.86 (t, J = 7.6 Hz, 2H), 3.83 (s, 3H), 4.22–4.27 (m, 2H), 4.57 (dq, J = 11.3, 4.7 Hz, 1H), 5.69 (brs, 1H), 5.99 (ddd, J = 9.7, 2.6, 1.1 Hz, 1H), 6.65 (dd, J = 8.0, 2.0 Hz, 1H), 6.68 (d, J = 1.9 Hz, 1H), 6.79 (d, J = 8.0 Hz, 1H), 6.84 ppm (ddd, J = 9.7, 5.7, 2.7 Hz, 1H); ¹³C NMR (151 MHz, CDCl₃): δ = 25.7, 30.6, 36.0, 55.9, 64.5, 75.2, 111.0, 114.4, 120.8, 121.1, 132.1, 144.2, 144.7, 146.6, 163.4, 172.6 ppm; IR (NaCl): $\tilde{\nu}$ = 1033, 1082, 1153, 1237, 1515, 1720, 2934, 3424 cm⁻¹ (broad); HRMS: m/z : calcd for C₁₆H₁₈O₆ + H⁺: 307.1182 [M + H]⁺; found: 307.1219.

General procedure for hydrogenation to produce saturated acids: Pd/C (5% w/w, 40 mg) was added to a solution of acid (0.92 mmol) in EtOAc (5 mL). The heterogeneous mixture was stirred under a hydrogen atmosphere for 3 h. The mixture was filtered through Celite, and the solvent was removed under reduced pressure.

3-(3,4-Bis[(*tert*-butyldimethylsilyloxy)phenyl]propanoic acid (31). Yield: 373 mg (99%). Pale-yellow solid; R_f = 0.54 (SiO₂, hexanes/EtOAc 75:25); mp: 88–89 °C; ¹H NMR (250 MHz, CDCl₃): δ = 0.18 (s, 12H), 0.98 (s, 18H), 2.62 (t, J = 7.5 Hz, 2H), 2.84 (t, J = 7.8 Hz, 2H), 6.60–6.78 ppm (m, 3H); ¹³C NMR (62.9 MHz, CDCl₃): δ = -3.95 (4C), 18.6 (2C), 26.1 (6C), 30.1, 36.1, 121.2 (2C), 121.3, 133.4, 145.4, 146.8, 179.7 ppm.

3-[4-[(*tert*-Butyldimethylsilyloxy)-3-methoxyphenyl]propanoic acid. Yield: 282 mg (99%). Pale-yellow solid; R_f = 0.50 (SiO₂, hexanes/EtOAc 60:40); mp: 39–43 °C; ¹H NMR (250 MHz, CDCl₃): δ = 0.13 (s, 6H), 0.98 (s, 9H), 1.89 (brs, 2H), 2.86 (brs, 2H), 3.74 (s, 3H), 6.58–6.77 ppm (m, 3H); ¹³C NMR (62.9 MHz, [D₄]methanol): δ = -4.3 (2C), 19.4, 26.4 (3C), 32.2, 38.2, 56.0, 113.7, 121.6, 121.8, 136.4, 144.5, 152.2, 178.5 ppm.

3-(3,4-Dimethoxyphenyl)propanoic acid. Yield: 191 mg (99%). White solid; R_f = 0.41 (SiO₂, hexanes/EtOAc 30:70); mp: 89–93 °C; ¹H NMR (250 MHz, CDCl₃): δ = 2.66 (t, J = 7.9 Hz, 2H), 2.91 (t, J = 7.9 Hz, 2H), 3.85 (s, 3H), 3.86 (s, 3H), 6.71–6.82 ppm (m, 3H); ¹³C NMR (62.9 MHz, CDCl₃): δ = 30.3, 36.0, 55.9, 56.0, 111.5, 111.8, 120.2, 132.9, 147.7, 149.0, 179.1 ppm.

(E)-3-[3,4-bis[(*tert*-Butyldimethylsilyloxy)phenyl]acrylic acid (32). Freshly distilled diisopropylethylamine (2.91 mL, 16.7 mmol, 5.0 equiv) and *tert*-butyldimethylsilyl chloride (2.09 g, 13.9 mmol, 5.0 equiv) were added to a suspension of caffeic acid (500 mg, 2.78 mmol, 1 equiv) in anhydrous CH₂Cl₂ (3.4 mL) at 25 °C; the mixture became a solution, which was stirred at 25 °C for 14 h. The mixture was diluted with EtOAc (15 mL), extracted with water (5 mL), and successively washed with an aqueous solution of 1 M HCl (2 × 10 mL) and brine (10 mL). Then, the organic phase was dried (MgSO₄) and concentrated to obtain a yellow oil. This oil was dissolved in THF (4 mL) and solid K₂CO₃ (400 mg) and water (0.7 mL) were added. The mixture was stirred for 2 h. Upon com-

pletion, the mixture was diluted with EtOAc (15 mL), extracted with water (10 mL), and successively washed with an aqueous solution of 1 M HCl (10 mL) and brine (10 mL). Then, the organic phase was dried (MgSO₄) and concentrated. The solid was dried under reduced pressure (1.0 kPa) at 60 °C for 4 h to obtain **32** as a pale-yellow solid (1.078 g, 95%); R_f = 0.40 (SiO₂, hexanes/EtOAc 75:25); mp: 157–160 °C; ¹H NMR (250 MHz, CDCl₃): δ = 0.22 (s, 6H), 0.23 (s, 6H), 0.99 (s, 9H), 1.00 (s, 9H), 6.24 (d, J = 15.8 Hz, 1H), 6.81–6.87 (m, 1H), 7.01–7.08 (m, 2H), 7.67 ppm (d, J = 16.0 Hz, 1H); ¹³C NMR (62.9 MHz, CDCl₃): δ = -4.0 (2C), -3.9 (2C), 18.6, 18.6, 26.0 (6C), 115.0, 120.8, 121.3, 122.9, 127.8, 147.2, 147.4, 150.1, 173.2 ppm.

(E)-3-[4-[(*tert*-Butyldimethylsilyloxy)-3-methoxyphenyl]acrylic acid. Freshly distilled diisopropylethylamine (5.38 mL, 30.9 mmol, 3 equiv) and *tert*-butyldimethylsilyl chloride (3.88 g, 25.8 mmol, 2.5 equiv) were added to a mixture of ferulic acid (2000 mg, 10.3 mmol, 1 equiv) in anhydrous CH₂Cl₂ (18 mL) at 25 °C, and the mixture was stirred for 14 h. Then, the mixture was diluted with EtOAc (25 mL), extracted with water (10 mL), and successively washed with an aqueous solution of 1 M HCl (2 × 15 mL) and brine (15 mL); the organic phase was dried (MgSO₄) and concentrated to obtain a yellow oil. This oil was dissolved in THF (10 mL) and solid K₂CO₃ (800 mg) and water (1 mL) were added. The mixture was stirred for 2 h. Upon completion, the mixture was diluted with EtOAc (20 mL), extracted with water (15 mL), and successively washed with an aqueous solution of 1 M HCl (15 mL) and brine (15 mL). The organic phase was dried (MgSO₄) and concentrated. The solid was dried under reduced pressure (1.0 kPa) at 60 °C for 4 h to obtain the acid as a pale-yellow solid (2.90 g, 95%); R_f = 0.46 (SiO₂, hexanes/EtOAc 60:40); mp: 188–190 °C; ¹H NMR (250 MHz, CDCl₃): δ = 0.14 (s, 6H), 0.98 (s, 9H), 3.72 (s, 3H), 6.34 (d, J = 15.3 Hz, 1H), 6.65–7.05 (m, 3H), 7.65 ppm (d, J = 15.3 Hz, 1H); ¹³C NMR (62.9 MHz, [D₄]methanol): δ = -4.3 (2C), 19.4, 26.3 (3C), 56.1, 112.2, 119.9, 122.1, 123.0, 130.5, 144.9, 148.3, 152.6, 173.1 ppm.

(E)-3-(3,4-Dimethoxyphenyl)acrylic acid. Dimethyl sulfate (4.6 mL, 48.6 mmol) was added to a mixture of ferulic acid (2.00 g, 10.3 mmol, 1 equiv) and potassium carbonate (13.0 g, 94 mmol, 9.1 equiv) in acetone (50 mL). The mixture was heated at reflux overnight, filtered through a short column of silica gel (EtOAc as eluent), and the solvent was evaporated under reduced pressure. The residue was dissolved in methanol (35 mL) and an aqueous solution of sodium hydroxide 10% w/v (35 mL). This mixture was heated at reflux for 3 h. The mixture was neutralized with an aqueous solution of 6 M HCl at 0 °C. The mixture was filtered, and the solid was washed with cold water. The solid was dried under reduced pressure (1.0 kPa) at 70 °C to produce the acid as a white solid (1.98 g, 92%); R_f = 0.46 (SiO₂, hexanes/EtOAc 30:70); mp: 178–180 °C; ¹H NMR (250 MHz, CDCl₃): δ = 3.93 (s, 6H), 6.33 (d, J = 16.0 Hz, 1H), 6.88 (d, J = 8.2 Hz, 1H), 7.08 (d, J = 1.4 Hz, 1H), 7.14 (dd, J = 8.2, 1.3 Hz, 1H), 7.73 ppm (d, J = 16.0 Hz, 1H); ¹³C NMR (62.9 MHz, CDCl₃): δ = 56.1 (2C), 110.0, 111.2, 115.1, 123.3, 127.2, 147.1, 149.4, 151.7, 172.7 ppm.

(Allyloxy)(*tert*-butyl)diphenylsilane (34). Imidazole (7.46 g, 109 mmol, 1.2 equiv) and *tert*-butyldiphenylsilyl chloride (30 mL, 115 mmol, 1.25 equiv) were added to a solution of allyl alcohol **33** (5.30 g, 91.2 mmol, 1.0 equiv) dissolved in anhydrous CH₂Cl₂ (182 mL) 0 °C. The temperature was increased to RT, and the mixture was stirred for 8 h; then, the solvent was removed under reduced pressure. The residue was poured into water (50 mL) and extracted with Et₂O (4 × 50 mL). The organic phases were combined, dried (MgSO₄), filtered, and concentrated under reduced pressure. The product was purified by column chromatography

(SiO₂, hexanes/EtOAc 95:5) to afford **34** as a colorless oil (27.0 g, quantitative yield): *R*_f=0.77 (SiO₂, hexanes/EtOAc 95:5); ¹H NMR (250 MHz, CDCl₃): δ = 1.08 (s, 9H), 4.20–4.24 (m, 2H), 5.12 (dd, *J* = 10.4, 1.7 Hz, 1H), 5.38 (dd, *J* = 17.1, 1.8 Hz, 1H), 5.86–6.02 (m, 1H), 7.35–7.47 (m, 6H), 7.67–7.73 ppm (m, 4H); ¹³C NMR (62.9 MHz, CDCl₃): δ = 19.3, 26.8 (3C), 64.6, 113.9, 127.6 (4C), 129.6 (2C), 133.7 (2C), 135.5 (4C), 137.0 ppm.

2-[(*tert*-Butyldiphenylsilyloxy)acetaldehyde (35). 2,6-Lutidine (10.7 mL, 9.84 g, 2.2 equiv), a solution of 2.5% w/w osmium tetroxide in *t*BuOH (235 mg of OsO₄, 0.02 equiv), and sodium periodate (39.5 g, 184 mmol, 4.4 equiv) were added to a solution of alkene **34** (12.5 g, 42.2 mmol, 1 equiv) in a mixture of water/1,4-dioxane (1:3 v/v, 500 mL). The mixture was stirred at RT for 24 h. Upon completion, the mixture was diluted with water (150 mL) and EtOAc (300 mL) and then filtered. The phases were separated, and the aqueous phase was extracted with EtOAc (2 × 300 mL). The organic phases were combined, washed with an aqueous solution of 1 M HCl (2 × 100 mL) and a saturated aqueous solution of NaHCO₃ (100 mL), and dried (MgSO₄). The solvent was removed under reduced pressure, and the product was purified by column chromatography (SiO₂, hexanes/EtOAc 95:5) to afford **35** as a brown oil (9.09 g, 72%): *R*_f=0.34 (SiO₂, hexanes/EtOAc 90:10); ¹H NMR (250 MHz, CDCl₃): δ = 1.14 (s, 9H), 4.24 (s, 2H), 7.36–7.51 (m, 6H), 7.66–7.77 (m, 4H), 9.74 ppm (s, 1H); ¹³C NMR (62.9 MHz, CDCl₃): δ = 19.4, 26.8 (3C), 70.1, 128.1 (4C), 130.2 (2C), 132.6 (2C), 135.6 (4C), 201.8 ppm.

(*S*)-1-[(*tert*-Butyldiphenylsilyloxy)pent-4-en-2-ol (36). A 50 mL round-bottomed flask containing a magnetic stir bar was charged with powdered activated 4 Å molecular sieves (2.5 g). After the addition of the molecular sieves, the flask was flame dried under flow of N₂. After this, anhydrous CH₂Cl₂ (6.4 mL), (*S*)-(–)-1,1'-bi-2-naphthol [(*S*)-BINOL; 189 mg, 0.66 mmol, 0.2 equiv], 1 M trifluoroacetic acid (TFA) in anhydrous CH₂Cl₂ (10 μL), and Ti(O*i*Pr)₄ (99 μL) were added. The mixture was heated at reflux for 1 h, at which point the color of the solution was observed to change dark red to brown. After this period, the oil bath was removed, the temperature was allowed to reach RT, and aldehyde **35** (994 mg, 3.33 mmol, 1.0 equiv) was added. The mixture was stirred for 15 min. The flask was placed in a bath at –78 °C and allyltributylstannane (1.6 mL, 4.98 mmol, 1.50 equiv) was added slowly to the mixture. The mixture was stirred at –20 °C for 4 days. After this period, brine (20 mL) was added to the mixture, and the temperature was allowed to reach RT. After 1 h, the mixture was filtered. The aqueous phase was extracted with CH₂Cl₂ (4 × 20 mL). The organic phases were grouped, dried (MgSO₄), filtered, and concentrated under reduced pressure. The product was purified by column chromatography (SiO₂, hexanes/EtOAc 90:10) to afford **36** as a colorless oil (988 mg, 87%): *R*_f=0.61 (SiO₂, hexanes/EtOAc 80:20); [α]_D²⁵ = –3 (*c* = 1.0 in CHCl₃). Lit.^[73] *ent*-compound [α]_D = +3 (*c* = 0.986 in CHCl₃); ¹H NMR (250 MHz, CDCl₃): δ = 1.07 (s, 9H), 2.15–2.29 (m, 3H), 3.55 (dd, *J* = 10.1, 7.0 Hz, 1H), 3.67 (dd, *J* = 10.1, 3.8 Hz, 1H), 3.73–3.85 (m, 1H), 5.02–5.14 (m, 2H), 5.80 (ddt, *J* = 17.1, 10.1, 7.0 Hz, 1H), 7.34–7.48 (m, 6H), 7.61–7.76 ppm (m, 4H); ¹³C NMR (62.9 MHz, CDCl₃): δ = 19.4, 27.0 (3C), 37.7, 67.4, 71.4, 117.6, 127.9 (4C), 129.9 (2C), 133.3 (2C), 134.4, 135.6 ppm (4C).

(*S*)-1-[(*tert*-Butyldiphenylsilyloxy)pent-4-en-2-yl acrylate (37). Freshly distilled triethylamine (0.46 mL, 3.28 mmol, 2.0 equiv) was added to a solution of alcohol **36** (560 mg, 1.64 mmol, 1.0 equiv) in anhydrous CH₂Cl₂ (8.2 mL) at 0 °C, and this was followed by the slow addition of acryloyl chloride (0.20 mL, 2.46 mmol, 1.5 equiv). The mixture was stirred for 1.5 h at RT. After this period, the solvent was removed and brine (10 mL) was added. The aqueous

phase was extracted with Et₂O (3 × 10 mL). The organic phases were grouped, dried (MgSO₄), filtered, and concentrated. The product was purified by column chromatography (SiO₂, hexanes/EtOAc 90:10) to afford **37** as a colorless oil (407 mg, 63%): *R*_f=0.71 (SiO₂, hexanes/EtOAc 80:20); [α]_D²⁵ = –5.7 (*c* = 1.0 in CHCl₃); Lit.^[74] *ent*-compound [α]_D = +8.3 (*c* = 0.986 in CHCl₃); ¹H NMR (250 MHz, CDCl₃): δ = 1.04 (s, 9H), 2.35–2.60 (m, 2H), 3.74 (d, *J* = 4.7 Hz, 2H), 5.00–5.19 (m, 3H), 5.65–5.89 (m, 2H), 6.04–6.19 (m, 1H), 6.35–6.46 (m, 1H), 7.33–7.48 (m, 6H), 7.62–7.72 ppm (m, 4H); ¹³C NMR (62.9 MHz; CDCl₃): δ = 19.4, 26.9 (3C), 35.2, 64.5, 73.8, 118.1, 127.8 (5C), 128.9, 129.8 (2C), 130.7, 133.5, 133.5, 135.7 (2C), 135.7 (2C), 165.7 ppm.

(*S*)-6-[(*tert*-Butyldiphenylsilyloxy)methyl]-5,6-dihydro-2H-pyran-2-one (38). Grubbs first-generation catalyst (112 mg, 0.14 mmol, 0.1 equiv) was added to a solution of acrylate **37** (535 mg, 1.4 mmol, 1.0 equiv) in CH₂Cl₂ (140 mL) at 40–45 °C. The mixture was heated at reflux for 6 h. After this time, DMSO (0.5 mL, 7.1 mmol, 5 equiv) was added at RT. The mixture was stirred for 12 h. Then, water (15 mL) was added. The phases were separated, and the organic material was extracted with water (5 × 15 mL). The organic phase was dried (MgSO₄) and concentrated. The product was purified by column chromatography (SiO₂, hexanes/EtOAc 70:30) to afford **38** as a brown oil (339 mg, 68%): *R*_f=0.37 (SiO₂, hexanes/EtOAc 70:30); [α]_D²⁵ = –38 (*c* = 1.5 in CHCl₃). Lit.^[75] *ent*-compound [α]_D = +34.2 (*c* = 1.5 in CHCl₃); ¹H NMR (250 MHz, CDCl₃): δ = 1.07 (s, 9H), 2.35–2.68 (m, 2H), 3.84 (d, *J* = 5.0 Hz, 2H), 4.52 (dq, *J* = 10.6, 4.9 Hz, 1H), 5.97–6.05 (m, 1H), 6.88 (ddd, *J* = 9.8, 5.5, 2.8 Hz, 1H), 7.35–7.55 (m, 6H), 7.62–7.70 ppm (m, 4H); ¹³C NMR (62.9 MHz, CDCl₃): δ = 19.3, 26.0, 26.9 (3C), 64.9, 77.7, 121.3, 127.9 (4C), 130.0 (2C), 132.9, 133.1, 135.7 (2C), 135.7 (2C), 145.0, 163.9 ppm.

(*S*)-6-(Hydroxymethyl)-5,6-dihydro-2H-pyran-2-one (39). A solution of 1 M TBAF in THF (1.14 mL, 1.14 mmol, 1.05 equiv) was added dropwise to a solution of lactone **38** (400 mg, 1.09 mmol, 1.0 equiv) and benzoic acid (139 mg, 1.14 mmol, 1.05 equiv) in anhydrous THF (55 mL) at 0 °C. The mixture was stirred for 4 h at RT, and then a saturated aqueous solution of NaHCO₃ (250 mL) was added. The mixture was extracted with EtOAc (7 × 200 mL), and the organic phases were grouped, dried (MgSO₄), filtered, and concentrated. The product was purified by column chromatography (SiO₂, EtOAc) to afford **39** as a colorless oil (126 mg, 90%): *R*_f=0.34 (SiO₂, EtOAc); [α]_D²⁵ = –159 (*c* = 1.0 in CHCl₃). Lit.^[14] *ent*-compound [α]_D = +160 (*c* = 0.85 in CHCl₃); ¹H NMR (400 MHz, CDCl₃): δ = 2.20 (brs, 1H), 2.26–2.36 (m, 1H), 2.55–2.66 (m, 1H), 3.74 (dd, *J* = 12.3, 4.8 Hz, 1H), 3.88 (dd, *J* = 12.3, 3.3 Hz, 1H), 4.55 (ddd, *J* = 12.3 Hz, 8.3, 4.0 Hz, 1H), 6.03 (ddd, *J* = 9.8, 2.8, 0.8 Hz, 1H), 6.93 ppm (ddd, *J* = 9.5, 6.3, 2.3 Hz, 1H); ¹³C NMR (62.9 MHz, CDCl₃): δ = 25.4, 64.0, 78.5, 121.1, 145.4, 163.9 ppm.

Biology

In vitro antiproliferative assay: Human tumor cell lines U-251 (glioma), MCF-7 (breast), NCI-H460 (lung, non-small cells), HT-29 (colon), PC-3 (prostate), 786-0 (kidney), and NCI-ADR/RES (ovarian expressing multiple drugs resistance phenotype) were obtained from the National Cancer Institute at Frederick, MA, USA. Human pancreatic cancer cells (Panc-1) were purchased from the Rio de Janeiro Cell Bank (Rio de Janeiro, RJ, Brazil). The non-tumor cell line HaCat (human keratinocytes) was donated by Prof. Dr. Ricardo Della Coletta, FOP/UNICAMP.

With the exception of Panc-1 cells, stock cultures were grown in RPMI 1640 (GIBCO BRL) medium supplemented with 5% fetal

bovine serum (FBS, GIBCO), 100 U mL⁻¹ penicillin, and 100 µg mL⁻¹ streptomycin at 37 °C with 5% CO₂. Panc-1 cells were cultured in DMEM (Nutricell, Brazil) containing 100 U mL⁻¹ penicillin, 100 µg mL⁻¹ streptomycin, and 10% FBS (GIBCO, Brazil) under the same conditions of temperature and atmosphere.

Cells in 96-well plates (100 µL cells well⁻¹) were exposed to tarcho-nanthuslactone and its analogues at concentrations 0.25, 2.5, 25, and 250 µg mL⁻¹ in DMSO/RPMI or DMEM at 37 °C, 5% CO₂, in air for 48 h. Doxorubicin was used as a positive control (0.025, 0.25, 2.5, and 25 µg mL⁻¹). The final DMSO concentration did not affect cell viability (0.1%). Afterward, cells were fixed with 50% trichloro-acetic acid, and cell proliferation was determined by spectropho-tometric quantification (540 nm) of cellular protein content by using the sulforhodamine B assay. The TGI (concentration that produces total growth inhibition or cytostatic effect) was determined through nonlinear regression analysis by using the concentration–response curve for each cell line (Table 1) in the ORIGIN 8.0 soft-ware (OriginLab Corporation).

Measurement of intracellular ROS production: Intracellular ROS levels were measured by flow cytometry in cells loaded with the redox-sensitive dye DCFH-DA (Sigma–Aldrich, St. Louis, MO, USA). Briefly, Panc-1 cells were washed with HBSS (Hank's buffered salt solution) medium and were incubated in the dark for 30 min at 37 °C with 10 µM DCFH-DA. Then, Panc-1 cells were treated with 25, 50, and 100 µM of compounds **8** and **9**. After 1 h of treatment, cells were harvested and resuspended in HBSS medium. Fluorescence was recorded with the FL-1 channel of a Guava Easycyte Mini flow cytometer (Guava Technologies, Hayward, CA). The data were analyzed with the software CytoSoft 4.1, Guava Express Pro program.

Measurement of apoptosis: Phosphatidylserine externalization was analyzed with the Guava Nexin Assay Kit (Guava Technologies, Hay-ward, CA) in accordance with the manufacturer's instructions. Panc-1 cells were treated with 25, 50, and 100 µM of compounds **8** and **9** for 24 h. Then, cells were harvested and resuspended at a density of 1 × 10⁵ cells in 100 µL of phosphate buffer saline (PBS). Binding buffer (100 µL) containing annexin-V and 7-AAD was added on the cells, which were then incubated in the dark for 20 min at room temperature. Thereafter, the cells were analyzed by flow cytometry (Guava Easycyte Mini, Guava Technologies, Hay-ward, CA).

Glutathione-S-transferase assay: Recombinant *S. japonicum* GST was produced in *E. coli* BL21DE3 by using the commercially available PGex vector (GE Life Sciences). Protein was purified by GSH-agar-ose (GE Life Sciences) affinity chromatography and eluted in a buffer containing 20 mM Tris (pH 7.5), 150 mM NaCl, and 5 mM GSH. Protein purity and ample quality were monitored by SDS-PAGE and dynamic light scattering. Protein concentration was measured by absorbance in a NanoDrop instrument by using the GST extinction coefficient of 42 860 M⁻¹ cm⁻¹ at λ = 280 nm. The purified protein was dialyzed in 50 mM Tris (pH 7.0) and 50 mM NaCl and concentrated to 1 mg mL⁻¹.

Enzyme activity was measured in the presence and absence of the test compounds by using GSH (0.7 mM) and 1-chloro-2,4-dinitro-benzene (CDNB, 2.5 mM) as substrates. The reaction buffer con-tained 100 mM Tris (pH 7.0), 0.01% Triton X-100, and 30 nM re-combinant GST. The enzyme was incubated with the tested com-pounds for 30 min at 20 °C prior to the addition of the substrates. Formation of the GSH–CDNB conjugate by the enzyme was moni-tored for 5 min at λ = 340 nm, 25 °C, by using an Envision (Perki-nElmer) plate reader. Blank experiments were conducted in the ab-

sence of the enzyme by using the same experimental conditions to account for possible non-enzymatic product formation. Stock solutions of the tested compounds were prepared in DMSO, which resulted in final DMSO concentration of 5% in the assay. A control group containing DMSO but not the inhibitors was conducted in parallel to represent 100% enzyme activity and was used to nor-malize the data. Initially, a single concentration (100 µM) of the in-hibitors was used to verify potential GST inhibitors in the series. Subsequently, concentration–response curves were conducted with the best inhibitors identified by using the concentration range of 1–100 µM. Enzyme initial velocities were calculated in the control and test groups. Data was normalized against the DMSO controls, plotted as percent of remaining enzyme activity versus the log of inhibitor concentration. Experimental curves were fitted by using the logistic four-parameter equation in the GraphPad software version 5 (GraphPad Prism, San Diego, CA, USA). Experi-ments were conducted in triplicate.

Protein phosphatase assays: The DNA sequence coding the human protein phosphatases PTP-1B, LMW-PTP, and CDC-25B were cloned into pET28a+ expression vectors and were expressed in *E. coli* BL-21DE3 with a 6-His N-terminal tag. The full-length sequence of LMW-PTP (UniProt code 24666) and the catalytic domains of CDC-25B (UniProt code P30305, isoform 3, residues 391–580) and PTP-1B (UniProt code P18031, residues 1–298) were selected. Expressed proteins were purified by Ni-affinity chromatography, followed by size-exclusion purification by using Superdex 75 resin (GE Life Sci-ences). Final buffers contained 100 mM Tris (pH 7.5), 150 mM NaCl, 1 mM dithiothreitol, and 10% glycerol. Samples were concentrated to 5–10 mg mL⁻¹ and were stored in liquid nitrogen. Protein con-centration was evaluated by using the method of Bradford.^[76] Pro-tein purity was checked by PAGE-SDS electrophoresis,^[77] and enzy-matic activity was confirmed with the *para*-nitrophenol phosphate (pNPP) activity assay.

IC₅₀ measurements were conducted by using the PTPase classic substrate pNPP, as previously reported.^[78–80] Assays were performed in 96-well plates by using an automated 8-channel pipet (Explor-er Eppendorf). Inhibitor stocks were prepared in DMSO, and enzymes were incubated with the tested compounds in the concentration range of 0.1–100 µM for 15 min at 30 °C in reaction buffer. The final DMSO concentration in each well was 5% in a total volume of 90 µL. Reaction buffers were adjusted to the ideal pH range for each PTPase and contained 100 mM sodium acetate (pH 5.5) and 0.005% Triton X-100 for LMW-PTP and PTP-1B and 100 mM bis-tris-propane (pH 8.2) and 0.005% Triton X-100 for CDC-25B. After the inhibitor incubation time, a 10 times stock solution containing the substrate was added. The final substrate concentration was in the range of the K_m value presented to each enzyme. The enzymatic reaction occurred over 10 min at 37 °C and was stopped by the ad-dition of 1 N NaOH (100 µL). Absorbance at λ = 405 nm, relative to pNP reaction product production, was measured in each well by using a M2e plate reader (Molecular Devices). Absorbance was nor-malized to the control group, which was measured under the same experimental conditions, however without the inhibitor (re-lated to 100% enzyme activity), and was plotted in a graph of in-hibitor concentration versus remaining enzyme activity. The experi-mental data were fit by using the logistic four-parameter equation in the GraphPad software version 5 (GraphPad Prism). At least two independent experiments conducted in triplicate were used for average and standard deviation calculation of the reported IC₅₀ values. Blank samples (in the absence of the enzyme) were also measured in each experiment to account for possible interference of the inhibitor in the absorbance measurement.

Reactive oxygen species detection in the enzymatic assays (FOX method): Detection of ROS in the protein phosphatase assays was performed by using the method of FOX (Fe²⁺/xylenol orange), according to the protocol used by Ogusucu et al.,^[69] adapted to microplates. The FOX reactant (100 μL) two times concentrated was added to the same volume of the phosphatase assays, which contained the phosphatase reaction buffer (0.5 mM Fe²⁺SO₄, 0.05 mM H₂SO₄, 0.2 mM xylenol orange, and 20 mM glucose) and the test compounds at 100 μM (in the absence of the phosphatase enzymes). The reaction was left for 15 min, and the absorbance at λ = 560 nm was measured by using a M2e microplate reader (Molecular Devices). Absorbance values were normalized to the values found in the DMSO controls and are expressed as the relative increase in ROS production. Experiments were conducted in duplicate.

Acknowledgements

The authors thank the Fundação de Amparo à Pesquisa do Estado de São Paulo (FAPESP) (research grants 2009/51602-5, 2010/17544-5, 2010/08673-6, 2012/09254-2, 2012/24385-6, and 2013/08896-3) and the Institute of Chemistry/UNICAMP for financial and academic support, and the Brazilian National Biosciences Laboratory for use of the Laboratory of Spectroscopy and Calorimetry (LEC). The authors also acknowledge Prof. Afonso C. D. Bairy and Jaco Mattos from the Federal University of Santa Catarina (Brazil) for their support in conducting initial analysis of the antioxidant enzymes.

Keywords: antitumor agents • cancer • natural products • reactive oxygen species • tarchonanthuslactone

- [1] J. Szychowski, J.-F. Truchon, Y. L. Bennani, *J. Med. Chem.* **2014**, *57*, 9292–9308.
- [2] J. Hong, *Chem. Eur. J.* **2014**, *20*, 10204–10212.
- [3] M. S. Butler, A. A. B. Robertson, M. A. Cooper, *Nat. Prod. Rep.* **2014**, *31*, 1612–1661.
- [4] J. A. Marco, M. Carda, J. Murga, E. Falomir, *Tetrahedron* **2007**, *63*, 2929–2958.
- [5] V. Boucard, G. Broustal, J. M. Campagne, *Eur. J. Org. Chem.* **2007**, 225–236.
- [6] A. de Fatima, L. Modolo, L. Conegero, R. Pilli, C. Ferreira, L. Kohn, *Curr. Med. Chem.* **2006**, *13*, 3371–3384.
- [7] Á. de Fátima, L. K. Kohn, J. E. de Carvalho, R. A. Pilli, *Bioorg. Med. Chem.* **2006**, *14*, 622–631.
- [8] M. Castaño, W. Cardona, W. Quiñones, S. Robledo, F. Echeverri, *Molecules* **2009**, *14*, 2491–2500.
- [9] M. J. Balunas, M. F. Grosso, F. A. Villa, N. Engene, K. L. McPhail, K. Tidgewell, *Org. Lett.* **2012**, *14*, 3878–3881.
- [10] S.-M. Lee, W.-G. Lee, Y.-C. Kim, Y.-C. Kim, H. Ko, *Bioorg. Med. Chem. Lett.* **2011**, *21*, 5726–5729.
- [11] T. A. Johnson, J. Sohn, A. E. Ward, T. L. Cohen, N. D. Lorig-Roach, H. Chen, *Bioorg. Med. Chem.* **2013**, *21*, 4358–4364.
- [12] T. Usui, H. Watanabe, H. Nakayama, Y. Tada, N. Kanoh, M. Kondoh, T. Asao, K. Takio, H. Watanabe, K. Nishikawa, T. Kitahara, H. Osada, *Chem. Biol.* **2004**, *11*, 799–806.
- [13] I. M. Serafimova, M. A. Pufall, S. Krishnan, K. Duda, M. S. Cohen, R. L. Maglathlin, *Nat. Chem. Biol.* **2012**, *8*, 471–476.
- [14] D. L. Boger, M. Hikota, B. M. Lewis, *J. Org. Chem.* **1997**, *62*, 1748–1753.
- [15] L. Bialy, H. Waldmann, *Chem. Eur. J.* **2004**, *10*, 2759–2780.
- [16] F. Bohlmann, A. Suwita, *Phytochemistry* **1979**, *18*, 677–678.
- [17] M. van Huyssteen, P. J. Milne, E. E. Campbell, M. van de Venter, *Afr. J. Tradit., Complementary Altern. Med.* **2011**, *8*, 150–158.
- [18] T. Nakata, H. Noriaki, I. Katsumi, O. Takeshi, *Tetrahedron Lett.* **1987**, *28*, 5661–5664.
- [19] Y. Mori, M. Suzuki, *J. Chem. Soc. Perkin Trans. 1* **1990**, 1809–1812.
- [20] G. Solladié, L. Gressot-Kempf, *Tetrahedron: Asymmetry* **1996**, *7*, 2371–2379.
- [21] M. V. R. Reddy, A. J. Yucel, P. V. Ramachandran, *J. Org. Chem.* **2001**, *66*, 2512–2514.
- [22] S. D. Garaas, T. J. Hunter, G. A. O'Doherty, *J. Org. Chem.* **2002**, *67*, 2682–2685.
- [23] D. Enders, D. Steinbusch, *Eur. J. Org. Chem.* **2003**, 4450–4454.
- [24] S. Baktharaman, S. Selvakumar, V. K. Singh, *Tetrahedron Lett.* **2005**, *46*, 7527–7529.
- [25] P. Gupta, S. V. Naidu, P. Kumar, *Tetrahedron Lett.* **2005**, *46*, 6571–6573.
- [26] G. Sabitha, K. Sudhakar, N. M. Reddy, M. Rajkumar, J. S. Yadav, *Tetrahedron Lett.* **2005**, *46*, 6567–6570.
- [27] M. S. Scott, C. A. Luckhurst, D. J. Dixon, *Org. Lett.* **2005**, *7*, 5813–5816.
- [28] S. George, A. Sudalai, *Tetrahedron: Asymmetry* **2007**, *18*, 975–981.
- [29] J. Yadav, P. Reddy, M. Gupta, C. Chary, *Synthesis* **2007**, 3639–3646.
- [30] J. S. Yadav, N. N. Kumar, M. S. Reddy, A. R. Prasad, *Tetrahedron* **2007**, *63*, 2689–2694.
- [31] H.-Y. Lee, V. Sampath, Y. Yoon, *Synlett* **2009**, 0249–0252.
- [32] G. F. P. de Souza, L. F. T. Novaes, C. M. Avila, L. F. R. Nascimento, L. A. Veloso, R. A. Pilli, *Molecules* **2015**, *20*, 5038–5049.
- [33] D. J. Adams, M. Dai, G. Pellegrino, B. K. Wagner, A. M. Stern, A. F. Shamji, *Proc. Natl. Acad. Sci. USA* **2012**, *109*, 15115–15120.
- [34] M. F. Tolba, A. Esmat, A. M. Al-Abd, S. S. Azab, A. E. Khalifa, H. A. Mosli, *IUBMB Life* **2013**, *65*, 716–729.
- [35] J.-Y. Lee, H.-J. Choi, T.-W. Chung, C.-H. Kim, H.-S. Jeong, K.-T. Ha, *J. Nat. Prod.* **2013**, *76*, 1399–1405.
- [36] R. Granata, L. Locati, L. Licitra, *Curr. Opin. Oncol.* **2013**, *25*, 224–228.
- [37] D. Seebach, M. Züger, *Helv. Chim. Acta* **1982**, *65*, 495–503.
- [38] G. E. Keck, K. H. Tarbet, L. S. Geraci, *J. Am. Chem. Soc.* **1993**, *115*, 8467–8468.
- [39] P. Kumar, P. Gupta, S. V. Naidu, *Chem. Eur. J.* **2006**, *12*, 1397–1402.
- [40] G. C. Vougioukalakis, R. H. Grubbs, *Chem. Rev.* **2010**, *110*, 1746–1787.
- [41] S. A. Snyder, F. Kontes, *J. Am. Chem. Soc.* **2009**, *131*, 1745–1752.
- [42] F. Bisogno, L. Mascoti, C. Sanchez, F. Garibotto, F. Giannini, M. Kurina-Sanz, *J. Agric. Food Chem.* **2007**, *55*, 10635–10640.
- [43] B. Narasimhan, D. Belsare, D. Pharande, V. Mourya, A. Dhake, *Eur. J. Med. Chem.* **2004**, *39*, 827–834.
- [44] A. Monks, D. Scudiero, P. Skehan, R. Shoemaker, K. Paull, D. Vistica, *J. Natl. Cancer Inst.* **1991**, *83*, 757–766.
- [45] L. V. Rubinstein, R. H. Shoemaker, K. D. Paull, R. M. Simon, S. Tosini, P. Skehan, *J. Natl. Cancer Inst.* **1990**, *82*, 1113–1118.
- [46] J. Liu, A. Mori, *Arch. Biochem. Biophys.* **1993**, *302*, 118–127.
- [47] R. C. Barcelos, J. C. Pastre, V. Caixeta, D. B. Vendramini-Costa, J. E. de Carvalho, R. A. Pilli, *Bioorg. Med. Chem.* **2012**, *20*, 3635–3651.
- [48] T. G. Hastings, M. J. Zigmond, *J. Neurochem.* **1994**, *63*, 1126–1132.
- [49] M. Brisson, C. Foster, P. Wipf, B. Joo, R. J. Tomko, Jr., T. Nguyen, J. S. Lazo, *Mol. Pharmacol.* **2007**, *71*, 184–192.
- [50] F. Puoci, C. Morelli, G. Cirillo, M. Curcio, O. I. Parisi, P. Maris, D. Sisci, N. Picci, *Anticancer Res.* **2012**, *32*, 2843–2847.
- [51] K. J. Pelizzaro-Rocha, M. B. de Jesus, R. R. Ruela-de-Sousa, C. V. Nakamura, F. S. Reis, A. de Fátima, *Biochim. Biophys. Acta Mol. Cell Res.* **2013**, *1833*, 2856–2865.
- [52] A. N. Shah, J. M. Summy, J. Zhang, S. I. Park, N. U. Parikh, G. E. Gallick, *Ann. Surg. Oncol.* **2007**, *14*, 3629–3637.
- [53] W. Huanwen, L. Zhiyong, S. Xiaohua, R. Xinyu, W. Kai, L. Tonghua, *Mol. Cancer* **2009**, *8*, 125.
- [54] T. H. Ward, J. Cummings, E. Dean, A. Greystoke, J. M. Hou, A. Backen, *Br. J. Cancer* **2008**, *99*, 841–846.
- [55] L. Galluzzi, I. Vitale, J. M. Abrams, E. S. Alnemri, E. H. Baehrecke, M. V. Blagosklonny, *Cell Death Differ.* **2012**, *19*, 107–120.
- [56] D. Trachootham, J. Alexandre, P. Huang, *Nat. Rev. Drug Discovery* **2009**, *8*, 579–591.
- [57] L. Raj, T. Ide, A. U. Gurkar, M. Foley, M. Schenone, X. Li, *Nature* **2011**, *475*, 231–234.
- [58] G. T. Wondrak, *Antioxid. Redox Signaling* **2009**, *11*, 3013–3069.
- [59] J. Luo, N. L. Solimini, S. J. Elledge, *Cell* **2009**, *136*, 823–837.
- [60] K. D. Tew, D. M. Townsend, *Curr. Opin. Chem. Biol.* **2011**, *15*, 156–161.
- [61] L. A. Sena, N. S. Chandel, *Mol. Cell* **2012**, *48*, 158–167.

- [62] M. Brisson, T. Nguyen, P. Wipf, B. Joo, B. W. Day, J. S. Skoko, E. M. Schreiber, C. Foster, P. Bansal, J. S. Lazo, *Mol. Pharmacol.* **2005**, *68*, 1810–1820.
- [63] L. Bialy, H. Waldmann, *Angew. Chem. Int. Ed.* **2005**, *44*, 3814–3839; *Angew. Chem.* **2005**, *117*, 3880–3906.
- [64] P. Chiarugi, P. Cirri, *Trends Biochem. Sci.* **2003**, *28*, 509–514.
- [65] P. Chiarugi, G. Pani, E. Giannoni, L. Taddei, R. Colavitti, G. Raugei, *J. Cell Biol.* **2003**, *161*, 933–944.
- [66] A. Salmeen, J. N. Andersen, M. P. Myers, T.-C. Meng, J. A. Hinks, N. K. Tonks, *Nature* **2003**, *423*, 769–773.
- [67] P. A. Ferreira, R. R. Ruela-de-Sousa, K. C. S. Queiroz, A. C. S. Souza, R. Milani, R. A. Pilli, *PLoS ONE* **2012**, *7*, e44312.
- [68] R. Ogusucu, D. Rettori, D. C. Munhoz, L. E. S. Netto, O. Augusto, *Free Radical Biol. Med.* **2007**, *42*, 326–334.
- [69] R. Ogusucu, D. Rettori, L. E. S. Netto, O. Augusto, *J. Biol. Chem.* **2009**, *284*, 5546–5556.
- [70] A. J. Barr, E. Ugochukwu, W. H. Lee, O. N. F. King, P. Filippakopoulos, I. Alfano, *Cell* **2009**, *136*, 352–363.
- [71] K. D. Tew, Y. Manevich, C. Grek, Y. Xiong, J. Uys, D. M. Townsend, *Free Radical Biol. Med.* **2011**, *51*, 299–313.
- [72] K. D. Tew, D. M. Townsend, *Drug Metab. Rev.* **2011**, *43*, 179–193.
- [73] Y. Díaz, F. Bravo, S. Castellón, *J. Org. Chem.* **1999**, *64*, 6508–6511.
- [74] A. Kamal, M. Balakrishna, P. V. Reddy, S. Faazil, *Tetrahedron: Asymmetry* **2010**, *21*, 2517–2523.
- [75] T. V. Hansen, *Tetrahedron: Asymmetry* **2002**, *13*, 547–550.
- [76] M. M. Bradford, *Anal. Biochem.* **1976**, *72*, 248–254.
- [77] U. K. Laemmli, *Nature* **1970**, *227*, 680–685.
- [78] Z.-Y. Zhang, J. C. Clemens, H. L. Schubert, J. A. Stuckey, M. W. Fischer, D. M. Hume, M. A. Saper, J. E. Dixon, *J. Biol. Chem.* **1992**, *267*, 23759–23766.
- [79] E. B. Gottlin, X. Xu, D. M. Epstein, S. P. Burke, J. W. Eckstein, D. P. Ballou, *J. Biol. Chem.* **1996**, *271*, 27445–27449.
- [80] F. Liu, D. E. Hill, J. Chernoff, *J. Biol. Chem.* **1996**, *271*, 31290–31295.

Received: June 3, 2015

Revised: August 3, 2015

Published online on August 25, 2015